Flame-enhanced laser-induced breakdown spectroscopy

Lei Liu, S. Li, X. N. He, Xi Huang, C. F. Zhang, Lisha Fan, M. X. Wang, Y. S. Zhou, K. Chen, Lan Jiang, et al.

Flame-enhanced laser-induced breakdown spectroscopy

L. Liu,[1] S. Li,[2] X. N. He,[1] X. Huang,[1] C. F. Zhang,[1] L. S. Fan,[1] M. X. Wang,[1] Y. S. Zhou,[1] K. Chen,[2] L. Jiang,[3] J. F. Silvain,[1,4] and Y. F. Lu[1,*]

[1]*Department of Electrical Engineering, University of Nebraska-Lincoln, Lincoln, NE 68588-0511, USA*
[2] *Department of Electrical and Computer Engineering, University of Pittsburgh, Pittsburgh, PA 15260, USA*
[3]*School of Mechanical Engineering, Beijing Institute of Technology, 100081, China*
[4]*Institut de Chimie de la Matière Condensée de Bordeaux – ICMCB-CNRS 87, Avenue du Docteur Albert Schweitzer F-33608 Pessac Cedex, France*
[*]*ylu2@unl.edu*

Abstract: Flame-enhanced laser-induced breakdown spectroscopy (LIBS) was investigated to improve the sensitivity of LIBS. It was realized by generating laser-induced plasmas in the blue outer envelope of a neutral oxy-acetylene flame. Fast imaging and temporally resolved spectroscopy of the plasmas were carried out. Enhanced intensity of up to 4 times and narrowed full width at half maximum (FWHM) down to 60% for emission lines were observed. Electron temperatures and densities were calculated to investigate the flame effects on plasma evolution. These calculated electron temperatures and densities showed that high-temperature and low-density plasmas were achieved before 4 μs in the flame environment, which has the potential to improve LIBS sensitivity and spectral resolution.

OCIS codes: (300.6365) Spectroscopy, laser induced breakdown; (350.5400) Plasmas.

References and links

1. W. M. Andrzej, P. Vincenzo, and S. Israel, *Laser-Induced Breakdown Spectroscopy: Fundamentals and Applications* (Cambridge University, 2006).
2. J. E. Carranza, B. T. Fisher, G. D. Yoder, and D. W. Hahn, "On-line analysis of ambient air aerosols using laser-induced breakdown spectroscopy," Spectrochim. Acta, B At. Spectrosc. **56**(6), 851–864 (2001).
3. A. Kumar, F. Y. Yueh, J. P. Singh, and S. Burgess, "Characterization of malignant tissue cells by laser-induced breakdown spectroscopy," Appl. Opt. **43**(28), 5399–5403 (2004).
4. M. D. Mowery, R. Sing, J. Kirsch, A. Razaghi, S. Béchard, and R. A. Reed, "Rapid at-line analysis of coating thickness and uniformity on tablets using laser induced breakdown spectroscopy," J. Pharm. Biomed. Anal. **28**(5), 935–943 (2002).
5. K. Y. Yamamoto, D. A. Cremers, M. J. Ferris, and L. E. Foster, "Detection of metals in the environment using a portable laser-induced breakdown spectroscopy instrument," Appl. Spectrosc. **50**(2), 222–233 (1996).
6. J. L. Gottfried, F. C. De Lucia, Jr., C. A. Munson, and A. W. Miziolek, "Laser-induced breakdown spectroscopy for detection of explosives residues: a review of recent advances, challenges, and future prospects," Anal. Bioanal. Chem. **395**(2), 283–300 (2009).
7. S. Tzortzakis, D. Anglos, and D. Gray, "Ultraviolet laser filaments for remote laser-induced breakdown spectroscopy (LIBS) analysis: applications in cultural heritage monitoring," Opt. Lett. **31**(8), 1139–1141 (2006).
8. V. I. Babushok, F. C. De Lucia, Jr., J. L. Gottfried, C. A. Munson, and A. W. Miziolek, "Double pulse laser ablation and plasma: Laser induced breakdown spectroscopy signal enhancement," Spectrochim. Acta, B At. Spectrosc. **61**(9), 999–1014 (2006).
9. D. K. Killinger, S. D. Allen, R. D. Waterbury, and C. Stefano, "Enhancement of Nd:YAG LIBS emission of a remote target using a simultaneous CO_2 laser pulse," Opt. Lett. **15**(20), 12905–12915 (2007).
10. J. Scaffidi, J. Pender, W. Pearman, S. R. Goode, B. W. Colston, Jr., J. C. Carter, and S. M. Angel, "Dual-pulse laser-induced breakdown spectroscopy with combinations of femtosecond and nanosecond laser pulses," Appl. Opt. **42**(30), 6099–6106 (2003).
11. X. K. Shen, J. Sun, H. Ling, and Y. F. Lu, "Spatial confinement effects in laser-induced breakdown spectroscopy," Appl. Phys. Lett. **91**(8), 081501 (2007).
12. A. M. Popov, F. Colao, and R. Fantoni, "Spatial confinement of laser-induced plasma to enhance LIBS sensitivity for trace elements determination in soils," J. Anal. At. Spectrom. **25**(6), 837–848 (2010).
13. L. B. Guo, C. M. Li, W. Hu, Y. S. Zhou, B. Y. Zhang, Z. X. Cai, X. Y. Zeng, and Y. F. Lu, "Plasma confinement by hemispherical cavity in laser-induced breakdown spectroscopy," Appl. Phys. Lett. **98**(13), 131501 (2011).

#204323 - $15.00 USD Received 8 Jan 2014; revised 16 Mar 2014; accepted 18 Mar 2014; published 26 Mar 2014

14. X. K. Shen, Y. F. Lu, T. Gebre, H. Ling, and Y. X. Han, "Optical emission in magnetically confined laser-induced breakdown spectroscopy," J. Appl. Phys. **100**(5), 053303 (2006).
15. Y. A. Liu, M. Baudelet, and M. Richardson, "Elemental analysis by microwave-assisted laser-induced breakdown spectroscopy: Evaluation on ceramics," J. Anal. At. Spectrom. **25**(8), 1316–1323 (2010).
16. W. D. Zhou, K. X. Li, Q. M. Shen, Q. L. Chen, and J. Long, "Optical emission enhancement using laser ablation combined with fast pulse discharge," Opt. Express **18**(3), 2573–2578 (2010).
17. X. N. He, W. Hu, C. M. Li, L. B. Guo, and Y. F. Lu, "Generation of high-temperature and low-density plasmas for improved spectral resolutions in laser-induced breakdown spectroscopy," Opt. Express **19**(11), 10997–11006 (2011).
18. D. N. Stratis, K. L. Eland, and S. M. Angel, "Effect of pulse delay time on a pre-ablation dual-pulse LIBS plasma," Appl. Spectrosc. **55**(10), 1297–1303 (2001).
19. R. Sanginés, H. Sobral, and E. Alvarez-Zauco, "The effect of sample temperature on the emission line intensification mechanism in orthogonal double-pulse laser induced breakdown spectroscopy," Spectrochim. Acta, B At. Spectrosc. **68**, 40–45 (2012).
20. S. Eschlböck-Fuchs, M. J. Haslinger, A. Hinterreiter, P. Kolmhofer, N. Huber, R. Rössler, J. Heitz, and J. D. Pedarnig, "Influence of sample temperature on the expansion dynamics and the optical emission of laser-induced plasma," Spectrochim. Acta, B At. Spectrosc. **87**, 36–42 (2013).
21. S. H. Tavassoli and A. Gragossian, "Effect of sample temperature on laser-induced breakdown spectroscopy," Opt. Laser Technol. **41**(4), 481–485 (2009).
22. M. A. Hafez, M. A. Khedr, F. F. Elaksher, and Y. E. Gamal, "Characteristics of Cu plasma produced by a laser interaction with a solid tartget," Plasma Sources Sci. Technol. **12**(2), 185–198 (2003).
23. D. H. Lee, S. C. Han, T. H. Kim, and J. I. Yun, "Highly sensitive analysis of boron and lithium in aqueous solution using dual-pulse laser-induced breakdown spectroscopy," Anal. Chem. **83**(24), 9456–9461 (2011).
24. H. R. Griem, *Spectral Line Broadening by Plasma* (Academic, 1974).

1. Introduction

Laser-induced breakdown spectroscopy (LIBS) has been a powerful and useful element analysis technique in recent years. This method is based on using a focused high power laser to induce plasmas on the target surface. The spectral analysis of the emission lines from the luminous plasma provides the elemental compositions of the target. Because the plasma is formed by focused laser irradiation, it has many advantages including the capability of multi-element detection, ability to detect solid, liquid and gas targets, no sample preparation, real-time and in situ analysis, nearly nondestructive measurements [1]. These advantages of LIBS offer a wide range of applications, such as aerosol analysis [2], biomedical analysis [3], pharmaceutical materials analysis [4], environment analysis [5,6], and cultural heritage objects analysis [7].

Many methods have been developed to improve the sensitivity of LIBS, such as, dual-pulse excitation [8–10], spatial or magnetic confinement [11–14], microwave-assisted LIBS [15], and laser ablation combined with fast pulse discharge [16]. Generation of high-temperature and low-density plasmas in LIBS to improve the spectral resolution has also been achieved by introducing a second laser pulse to re-ablate the laser-induced particles with delays up to milliseconds [17]. These high-temperature and low-density plasmas have the potential of spectral resolution improvement.

In our study, such plasmas were generated in the blue outer envelope of a neutral oxy-acetylene flame to improve the LIBS sensitivity. Fast imaging and temporally resolved spectroscopy were carried out to study the plasma evolution. Electron temperatures and densities were calculated to investigate the flame effects on the plasmas.

2. Experimental methods

2.1 Experimental setup

The schematic experimental setup for the flame-enhanced LIBS is shown in Fig. 1. The laser used for plasma generation was a pulsed KrF excimer laser (Lambda Physik, Compex 205 F) with a wavelength of 248 nm and a pulse duration of 23 ns. The laser was operated in the external triggered mode for synchronization. The laser beam was normally focused onto the target surface by an ultraviolet (UV) grade quartz lens (Lens 1 with a 20-cm focal length) to a spot size of about $2\times 0.8\,\mathrm{mm}^2$ with a fluence of 3.3 J/cm^2. The target was mounted on a

#204323 - $15.00 USD Received 8 Jan 2014; revised 16 Mar 2014; accepted 18 Mar 2014; published 26 Mar 2014

slowly rotating motor to avoid over ablation. A commercial oxygen-acetylene torch with a 1.5 mm orifice tip was used to generate the flame. The fuel was a mixture of ethylene (C_2H_4) and acetylene (C_2H_2) with a gas flow ratio of 1:1, which was then mixed with oxygen (O_2) with a volume ratio of 1.03 [(C_2H_{4+} C_2H_2)/O_2]. The plasmas were generated in the blue outer envelope of this neutral oxyacetylene flame with the envelope temperature around 1260 °C. The laser absorption by the flame was negligible. An aluminum alloy target (NIST 1255b) with an aluminum content of 91% and a low alloy steel target (NIST 1762) were used in this study.

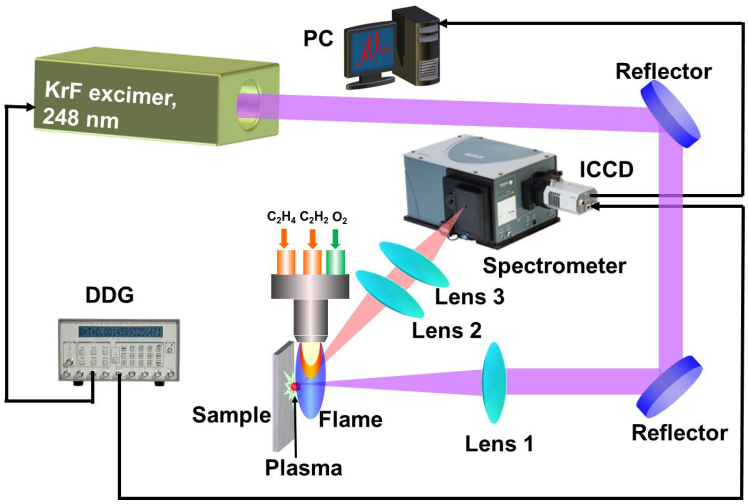

Fig. 1. Schematic experimental setup for flame-enhanced assisted LIBS.

2.2 Spectral measurements

The optical emission from plasmas was coupled into a spectrometer (Andor Tech., Shamrock 303i) by lens 2 (5-cm focal length) and lens 3 (10-cm focal length). The spectral resolution for the 2400-line grating is 0.05 nm. A 512 × 512 pixel intensified CCD detector (ICCD: Andor Tech., iStar, DH-712) was attached to the exit focal plane of the spectrometer. The ICCD detector was operated in the gate mode. The gate delay and gate width can be adjusted so that the spectra at different time delays after the laser pulse can be obtained. All the spectra were accumulated for 50 pulses to reduce the standard deviation in this study. Both the spectrometer and laser were synchronized by a digital delay generator (Stanford Research System DG 535, 5 ps delay resolution). To better observe the plasma evolution process and avoid overexposure of ICCD, a small gate width (50 ns) was used to observe the plasma evolution before 2 μs and a larger gate width (200 ns) was used to observe the plasma evolution after that.

3. Results and discussion

3.1 Fast imaging and temporally resolved spectroscopy of plasmas with time delays below 2 μs

The aluminum alloy sample (NIST 1255b) was used to study the influence of flame on plasma evolution. Figure 2 shows the fast images of Al plasmas on a relative intensity scale without (top row) and with (bottom row) the presence of the flame in a time period of 0.8 ~2 μs. The

#204323 - $15.00 USD Received 8 Jan 2014; revised 16 Mar 2014; accepted 18 Mar 2014; published 26 Mar 2014

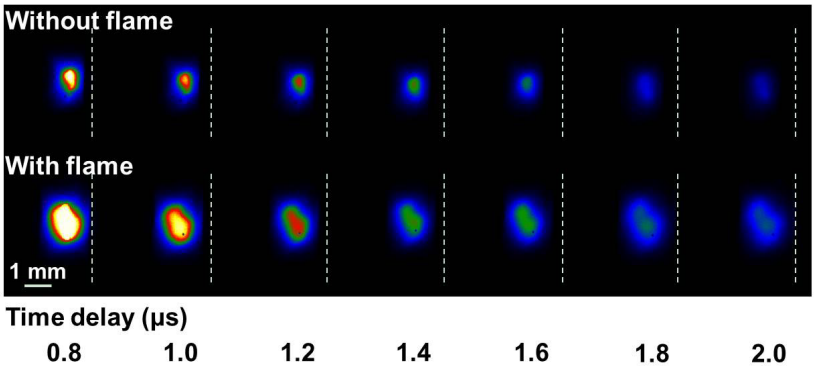

Fig. 2. Fast images of laser-induced Al plasmas in the time period of 0.8 ~2 μs without (top row) and with (bottom row) the presence of flame with a gate width of 50 ns and a laser fluence of 3.3 J/cm^2. The dash line shows the location of the sample surface.

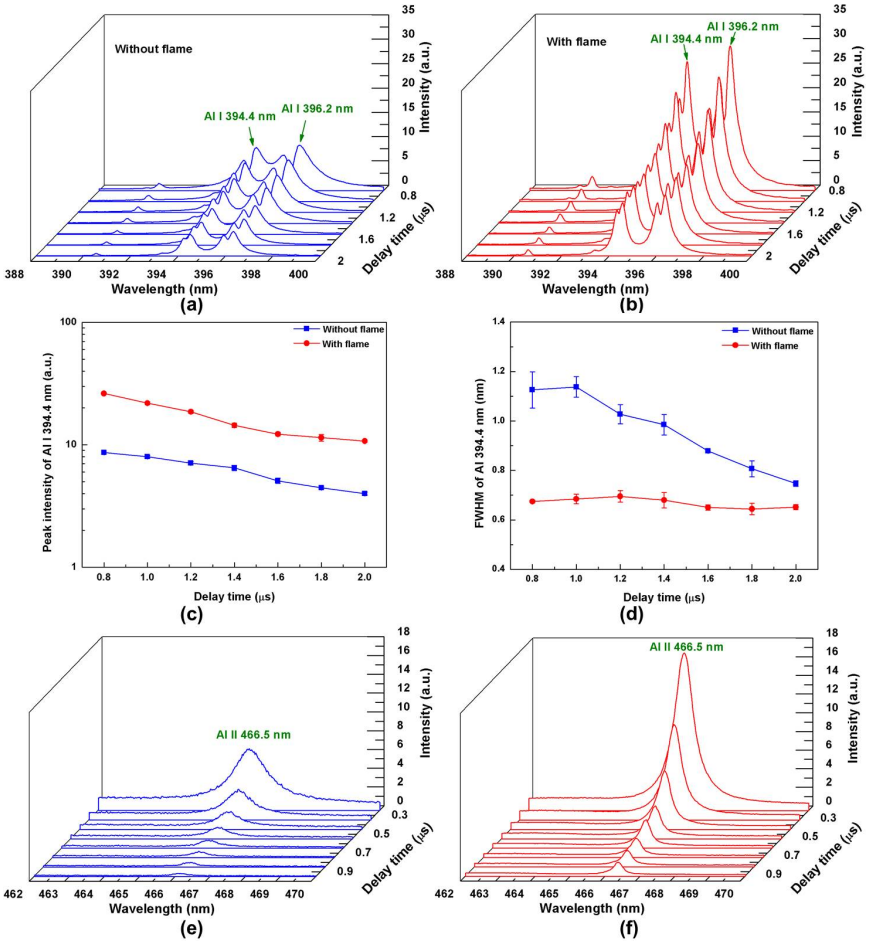

Fig. 3. Temporal evolution of Al spectra in the range of 388 ~400 nm (**a**) without flame (blue curve), (**b**) with flame (red curve); Al I 394.4 nm (Al atomic line) (**c**) peak intensity, and (**d**) FWHM evolution without (square blue curve) and with (dot red curve) flame; Temporal evolution in the spectral range of 462~470 nm (**e**) without flame (blue curve), (**f**) with flame (red curve) with a gate width of 50 ns and a laser fluence of 3.3 J/cm^2.

#204323 - $15.00 USD Received 8 Jan 2014; revised 16 Mar 2014; accepted 18 Mar 2014; published 26 Mar 2014

dash line shows the location of the sample surface. The first image was taken at a time delay of 0.8 μs with a gate width of 50 ns. The following images were taken with increasing time delays with a step of 200 ns. As shown in Fig. 2, the plasma plumes are always larger and brighter in the flame, which is primarily due to the fact that the plasmas have larger expansion rate in a hotter environment [18, 19]. Another factor contributed to this is the higher ablation rate caused by the higher sample temperature due to the flame heating [20, 21].

The Al atomic lines in the spectral range of 388 ~400 nm and Al ionic lines in the spectral range of 462 ~470 nm were measured to investigate the flame effects on these emission lines. Figures 3(a) and 3(b) show the temporal evolution of Al spectra in the range of 388 ~400 nm without and with flame in the time period of 0.8 ~2 μs, respectively. The first spectrum was acquired with a delay time of 0.8 μs. The following spectra were acquired with increasing delays with a step of 200 ns and a gate width of 50 ns. It is observed that the emission line intensities are always enhanced in the flame. Figures 3(c) and 3(d) show the temporal evolution of peak intensity and FWHM of the Al I 394.4 nm atomic line without (square blue curve) and with (dot red curve) the presence of the flame, respectively. The transition configuration for this Al I 394.4 nm atomic line is $3s^2 3p$ - $3s^2 4s$, where $3s^2 3p$ is the ground state of the Al atom. It is observed that in the flame environment, the peak intensity of the Al I 394.4 nm atomic line is enhanced for around 4 times while the FWHM is narrowed down to 60% at 0.8 μs.

The influence of the flame on the Al ionic lines was also investigated. Figures 3(e) and 3(f) show the temporal evolution of Al spectra in the range of 462 ~470 nm without and with the presence of flame, respectively, which mainly include the Al ionic line Al II 466.5 nm (Al II 466.3 and Al II 466.7 nm). The first spectrum was acquired with a delay time of 0.3 μs and a gate width of 50 ns. The following spectra were acquired with increasing delays with a step of 200 ns. The transition configuration for Al II 466.3 nm and Al II 466.7 nm are $3p^2$ - 3s4p and 3s5p - 3s11s, respectively. The intensity of the Al II 466.5 nm ionic line is enhanced for up to 3 times in the flame.

3.2 Fast imaging and temporally resolved spectroscopy of plasmas with time delays above 2 μs

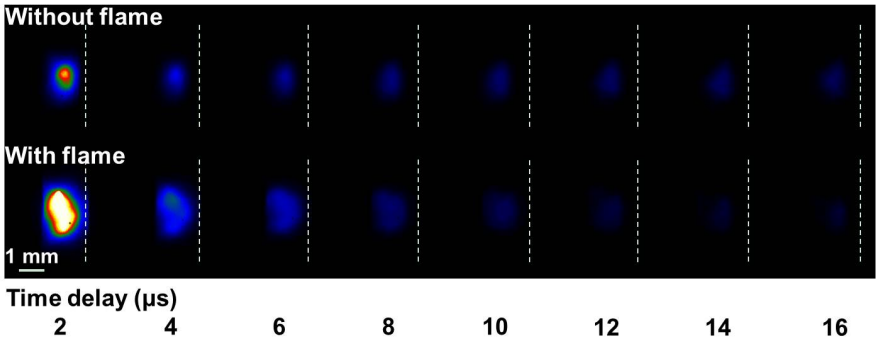

Fig. 4. Fast images of laser-induced Al plasmas in the time period of 2~16 μs without (top row) and with (bottom row) the presence of flame with a gate width of 200 ns and a laser fluence of 3.3 J/cm^2. The dash line shows the location of the sample surface.

In addition to the flame effects on Al plasmas in their early lifetime (before 2 μs) as described in the previous section, the flame effects on Al plasmas evolution after 2 μs were also investigated. Figure 4 shows the fast images of Al plasmas on a relative intensity scale without (top row) and with (bottom row) the flame from 2 to 16 μs. The dash line shows the location of the sample surface. The first image was acquired at a delay time of 2 μs with a gate width of 200 ns. The following images were acquired with increasing delays with a step

#204323 - $15.00 USD Received 8 Jan 2014; revised 16 Mar 2014; accepted 18 Mar 2014; published 26 Mar 2014

of 2 μs. As shown in Fig. 4, the plasma plume size is always larger in the flame. However, the brightness of the plasmas is stronger before 12 μs and weaker after that in the flame.

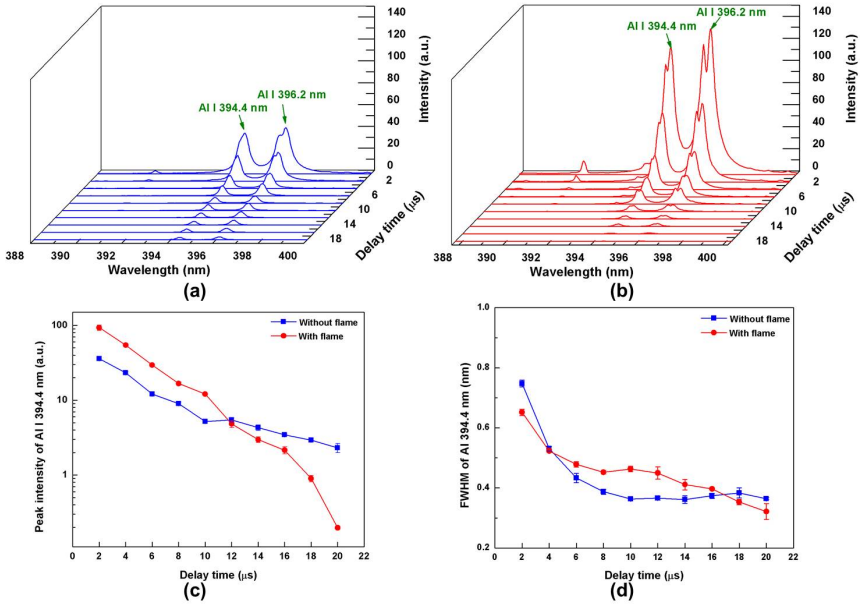

Fig. 5. Temporal evolution of Al spectra in the range of 388 ~400 nm (**a**) without flame (blue curve), (**b**) with flame (red curve); Al I 394.4 nm (Al atomic line) (**c**) peak intensity and (**d**) FWHM evolution without flame (square blue curve) and with (dot red curve) with a gate width of 500ns and a laser fluence of 3.3 J/cm^2.

Figures 5(a) and 5(b) show the temporal evolution of Al spectra in the range of 388 ~400 nm without and with the presence of flame in the time period of 2 ~20 μs, respectively. The first spectrum was acquired with a delay time of 2 μs and a gate width of 500 ns. The following spectra were acquired with increasing delays with a step of 2 μs. As observed, the emission line intensity is significantly enhanced with flame at the delay time of 2 μs. To better investigate the flame effect on the spectra evolution, the temporal evolution of peak intensity and FWHM of the Al I 394.4 nm atomic line were plotted in Figs. 5(c) and 5(d), respectively. As shown in Fig. 5(c), the peak intensities are enhanced before 12 μs but weakened after that in the flame. The peak intensities also decay rapidly in the flame, which results in a shorter plasma lifetime. As shown in Fig. 5(d), the FWHM of Al I 394.4 nm is also narrowed down to 86% at 2 μs with the flame, which indicates an improvement in the spectral resolution.

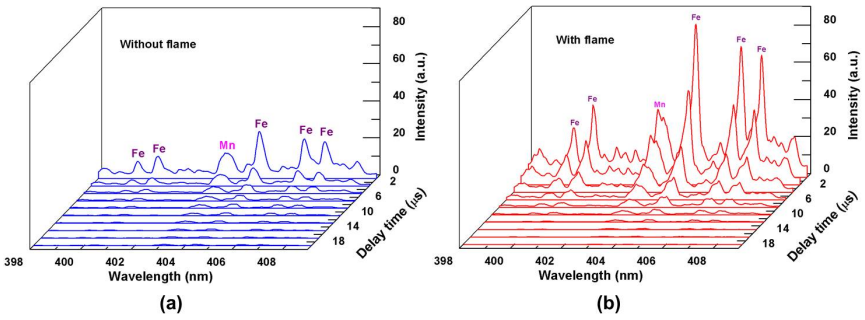

Fig. 6. Temporal evolution of the low steel alloy (NIST 1762) spectra in the range of 398 ~410 nm (**a**) without flame (blue curve), and (**b**) with flame (red curve) with a gate width of 500 ns and a laser fluence of 3.3 J/cm^2.

#204323 - $15.00 USD Received 8 Jan 2014; revised 16 Mar 2014; accepted 18 Mar 2014; published 26 Mar 2014

A low alloy steel target (NIST 1762) was also used to support the universality of the signal enhancement caused by flame on different elements in LIBS. Figures 6(a) and 6(b) show the temporal evolution of the low alloy steel spectra in the range of 398 ~410 nm without and with flame from 2 to 20 μs, respectively. At the delay time of 2 μs, the enhancement is up to 3 times for the detected elements with flame, including the low concentration elements such as manganese with a concentration of 2.00%. Furthermore, the emission line intensities decrease rapidly and are weaker after 12 μs in the flame, which is consistent with the results found in the previous Al plasmas experiments.

For the LIBS enhancement with the flame, the main factor is that the plasma temperature is higher before 8 μs in the flame, which causes more atoms to be excited. A minor factor is the larger ablation rate caused by the higher sample temperature due to the flame heating [19–21]. The shorter plasma lifetime is caused by the enhancement of energy transfer due to the increased collision among particles with the presence of the flame [22, 23].

3.3 Plasma temperature and density

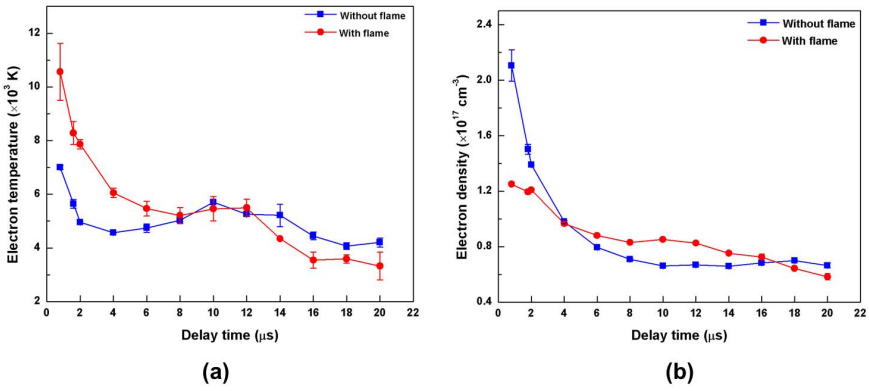

Fig. 7. Temporal evolution of Al electron (**a**) temperature and (**b**) density without (square blue curve) and with (circle red curve) flame.

The flame effects on the temporal evolution of the electron temperature and density of the Al plasmas are shown in Figs. 7(a) and 7(b), respectively. According to the local thermodynamic equilibrium assumption, plasma temperatures can be deduced from the relative intensities ratio of the spectral lines from the same element ionization stage [1, 24]. The lines selected for the calculation of the electron temperatures are Al I 308.22 nm and Al I 394.40 nm in this study. As shown in Fig. 7(a), the electron temperature rose by around 3000 K at 2 μs and was always higher before 8 μs with the flame. The electron density of Al plasmas was deduced from the Stark broadening of the Al I 394.4 nm line [1]. As shown in Fig. 7(b), the electron density decreased from ~2.1×10^{17} to ~1.3×10^{17} cm^{-3} at 1 μs. Thus, the plasmas have higher temperatures and lower densities before 4 μs, which are beneficial to enhancing optical emission intensity and improving spectral resolution since more excited atoms and less stark broadening effect could be obtained in higher temperatures and lower density plasmas.

4. Conclusions

The flame-enhanced laser-induced breakdown spectroscopy was studied to improve the LIBS sensitivity and spectral resolution by generating the laser-induced plasmas in the blue outer envelope of a neutral oxy-acetylene flame. Fast images and temporal spectral evolution were studied to investigate the flame effects on the plasma evolution. In the flame environment, both the atomic and ionic lines were enhanced up to 4 and 3 times respectively; the electron temperature rose by around 3000 K at 2 μs and the electron density decreased from ~2.1×10^{17} to ~1.3×10^{17} cm^{-3} at 1 μs; a high-temperature and low-density plasma was generated

#204323 - $15.00 USD Received 8 Jan 2014; revised 16 Mar 2014; accepted 18 Mar 2014; published 26 Mar 2014

with the FWHM of Al I 394.4 nm line narrowed down to 60% at 0.8 μs. Both the enhanced emission line intensity and narrowed FWHM were also found in a low alloy steel target. Flame-enhanced LIBS has the potential to improve the measurement sensitivity and spectral resolution in LIBS analysis.

Acknowledgments

This research work was financially supported by Defense Threat Reduction Agency (through HDTRA1-12-1-0019) and National Science Foundation (CMMI 0900419).

#204323 - $15.00 USD Received 8 Jan 2014; revised 16 Mar 2014; accepted 18 Mar 2014; published 26 Mar 2014